



Since January 2020 Elsevier has created a COVID-19 resource centre with free information in English and Mandarin on the novel coronavirus COVID-19. The COVID-19 resource centre is hosted on Elsevier Connect, the company's public news and information website.

Elsevier hereby grants permission to make all its COVID-19-related research that is available on the COVID-19 resource centre - including this research content - immediately available in PubMed Central and other publicly funded repositories, such as the WHO COVID database with rights for unrestricted research re-use and analyses in any form or by any means with acknowledgement of the original source. These permissions are granted for free by Elsevier for as long as the COVID-19 resource centre remains active.



Independent association of meteorological characteristics with initial spread of Covid-19 in India



Hemant Kulkarni ^{a,b,*}, Harshwardhan Khandait ^{c,1}, Uday W. Narlawar ^{a,c}, Pragati Rathod ^c, Manju Mamtani ^{a,b}

^a Lata Medical Research Foundation, Nagpur, India

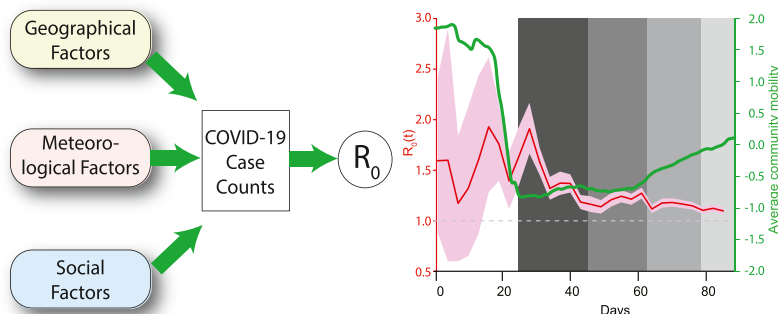
^b M&H Research, LLC, San Antonio, TX, USA

^c Government Medical College, Nagpur, India

HIGHLIGHTS

- We tested association of geo-socio-meteorological factors with COVID-19 in India.
- Air temperature, wind speed and lockdown were independently associated with R_0 .
- Countrywide lockdown contributed to COVID-19 more strongly than weather factors.

GRAPHICAL ABSTRACT



ARTICLE INFO

Article history:

Received 29 July 2020

Received in revised form 28 September 2020

Accepted 29 September 2020

Available online 16 October 2020

Editor: SCOTT SHERIDAN

Keywords:

Temperature

Wind speed

COVID-19

Basic reproduction rate

ABSTRACT

Whether weather plays a part in the transmissibility of the novel Coronavirus Disease-19 (COVID-19) is still not established. We tested the hypothesis that meteorological factors (air temperature, relative humidity, air pressure, wind speed and rainfall) are independently associated with transmissibility of COVID-19 quantified using the basic reproduction rate (R_0). We used publicly available datasets on daily COVID-19 case counts (total $n = 108,308$), three-hourly meteorological data and community mobility data over a three-month period. Estimated R_0 varied between 1.15 and 1.28. Mean daily air temperature (inversely), wind speed (positively) and countrywide lockdown (inversely) were significantly associated with time dependent R_0 , but the contribution of countrywide lockdown to variability in R_0 was over three times stronger as compared to that of temperature and wind speed combined. Thus, abating temperatures and easing lockdown may concur with increased transmissibility of COVID-19 in India.

© 2020 Elsevier B.V. All rights reserved.

1. Introduction

As the novel Coronavirus Disease-19 (COVID-19) continues to devastate the world, there remains a myriad of unknowns about its

pathogenesis, population dynamics, epidemiology, prevention and treatment. Since its introduction into the global susceptible population SARS-CoV-2, the causative agent of COVID-19, has presented several conundrums. It was initially believed that like many other viruses, SARS-CoV-2 may also be responsive to the environmental influences posed by climatic and meteorological factors (Adhikari and Yin, 2020; Briz-Redon and Serrano-Aroca, 2020; Qi et al., 2020; Tosepu et al., 2020). However, current understanding of the potential role of weather on the spread of SARS-CoV-2 is far from clear.

* Corresponding author at: 12023 Waterway Rdg, San Antonio, TX, USA.

E-mail address: hemant.kulkarni@mnhrsearch.com (H. Kulkarni).

¹ These authors contributed equally to this article.

The COVID-19 outbreaks have been generally more severe in the countries located in the mid-latitudes where the temperature is considerably low in contrast to the tropical countries. Several studies around the world have attempted to specifically establish a relationship between COVID-19 transmission and various meteorological factors (Brassley et al., 2020; Prata et al., 2020; Vantarakis et al., 2020). For example, a study conducted in New York, United States of America, found that mean temperature, minimum temperature and air quality were significantly associated with COVID-19 (Prata et al., 2020). Similarly, others have (Shi et al., 2020) reported a statistically significant correlation between daily temperature and daily count of COVID-19 cases in China and suggested that temperatures above 8–10 °C would lead to a decline in the number of infected cases. In a parallel investigation (Prata et al., 2020), it was concluded that a rise in 1 °C temperature would result in a 5% decrease in the number of daily confirmed COVID-19 cases in Brazil. There have been very few investigations (Das and Chatterjee, 2020; Gupta and Pradhan, 2020; Singh and Agarwal, 2020) from India in this regard – a country with second largest population size after China. These studies from India have generally indicated a potential role of weather conditions in the spread of COVID-19.

On the other end of the spectrum, a recent study (Yao et al., 2020) concluded that there is no association of COVID-19 transmission with temperature or ultraviolet (UV) radiation in Chinese cities. Indeed, an elegant, evidence-based review (Brassley et al., 2020) summarized the existing evidence in this regard and observed that a) cold and dry conditions may facilitate the spread of the novel coronavirus (SARS-CoV-2) b) much of the emerging data for SARS-CoV-2 has yet to be peer-reviewed and is thus needed; and c) relying on weather changes alone to slow the transmission of COVID-19 are unlikely to be sufficient. Considering these recommendations, the variability in the observed associations and a relative lack of such studies from India, we conducted this investigation on a nationwide sample of geographical locations across India. The primary goal was to test the putative association of geo-meteorological characteristics with COVID-19 transmission and to test its independence from other socio-behavioral interventions like lockdowns and social mobility.

2. Materials and methods

2.1. Data sources

We selected a total of 46 geographical locations across India. For each selected location (either a city, union territory or district), we collected data for a three-month period (March 1, 2020 through May 31, 2020). Following data items were collected for each study location: daily number of confirmed COVID-19 cases, meteorological data, demographic data and geographic data. The meteorological data included 3-hourly recordings of air temperature, relative humidity, air pressure, wind speed and rainfall. The demographic data included the 2011 census population and the geographical data included area and elevation. The area and population records were combined to estimate the population density. Lastly, temporal data on the lockdown implementation phases and the mobility of the population (estimated anonymously from the cellphone use data) was collected to study the potential temporal concurrence with COVID-19 transmission.

All data used in this study are publicly available and are completely anonymized. The study was approved by the Institutional Ethics Committee of Government Medical College, Nagpur, India. Following were the sources of data: number of daily COVID-19 cases – <https://api.covid19india.org/>; meteorological data – <https://www.tutiempo.net/> and <https://www.worldweatheronline.com/>; 2011 census data – <https://censusindia.gov.in/2011-common/censusdata2011.html>; and geographical data – combination of census data and search on Wikipedia® (<https://en.wikipedia.org/wiki/Wikipedia>). Lastly, the temporal mobility data was downloaded from the publicly available

repository: <https://www.google.com/covid19/mobility/>. These data reported percent change from baseline mobility on visits to the following five destinations – retail and recreation, grocery and pharmacy, parks, transit stations and workplaces.

2.2. Quantification of COVID-19 transmissibility

Using the daily case count data, we estimated the basic reproduction rate (R_0) in two different ways. First, we estimated the average R_0 over the entire duration of 92 days period of data collection. For this, we used two methods – the exponential growth (EG) and the maximum likelihood (ML). Second, we estimated the daily R_0 in a time-dependent (TD) fashion. All estimates of R_0 require a knowledge of serial interval, the time difference between onset of symptoms in an infector and an infectee. We assumed a gamma distributed serial interval with a mean of 3.96 days and a standard deviation of 4.75 days (Du et al., 2020). We used the R package R_0 (Obadia et al., 2012) to derive all the estimates of R_0 . Finally, we considered the possibility of biased estimates of R_0 owing to the relative lack of testing facilities, especially during the initial period of the epidemic. For this, we used the algorithmic method (Lachmann et al., 2020) that considers South Korea as the reference country and estimates the degree of undertesting by combining demographic and vital statistics data. Using this method, we derived the possible undertesting on each study day.

2.3. Statistical analysis

Our analyses used estimates of R_0 as the dependent variable and the geo-meteorological and socio-behavioral characteristics as the explanatory variables. To compare groupwise means we used the Mann-Whitney U test or Kruskal-Wallis test as appropriate. Significance of heterogeneity across study locations was statistically tested using the Q test. Time series data were smoothed using a five-day sliding window. Further, to make the different time series (each meteorological characteristic) comparable, we converted them to a series of z -scores. To test the temporal concurrence, we used the cross-correlation between two time series (Pearson's correlation). To test the association of time series variables with estimated time dependent R_0 , we used multivariable, ordinary least squares regression. Starting with the full model, we conducted stepwise, backward elimination regression modeling with a probability retention criterion of 0.05. Lastly, to quantify the relative contribution of each covariate with time dependent R_0 , we estimated the proportional reduction in error (PRE) using an established approach (Judd et al., 2009). PRE was estimated as reduction in the residual sum of squares by including a covariate in the full model. Statistical analyses were conducted using the Stata 14.2 statistical package (Stata Corp, College Station, TX). Type 1 error rate of 0.05 was used for hypothesis testing.

3. Results

3.1. Representativeness of the study locations

We included 46 locations across India that contained 32 cities, 12 districts and 2 union territories. Fig. 1 shows the geographical spread of these locations and the geographic and demographic details for these locations are provided in Table 1. The study locations varied widely in terms of the area (range 12.59–15,641 km²), elevation (range 1–3505 m above sea level) and population density (range 10 to 35,439/km²). The selected locations are distributed across India and represent majority of the states/union territories of India. Meteorological data was available on all the selected study locations.

The cumulative number of COVID-19 confirmed cases (till and including May 31, 2020) reported from these locations also varied widely (1 to 37,666). The 46 selected locations together accounted for a total of 108,308 confirmed COVID-19 cases. From entire India the number of

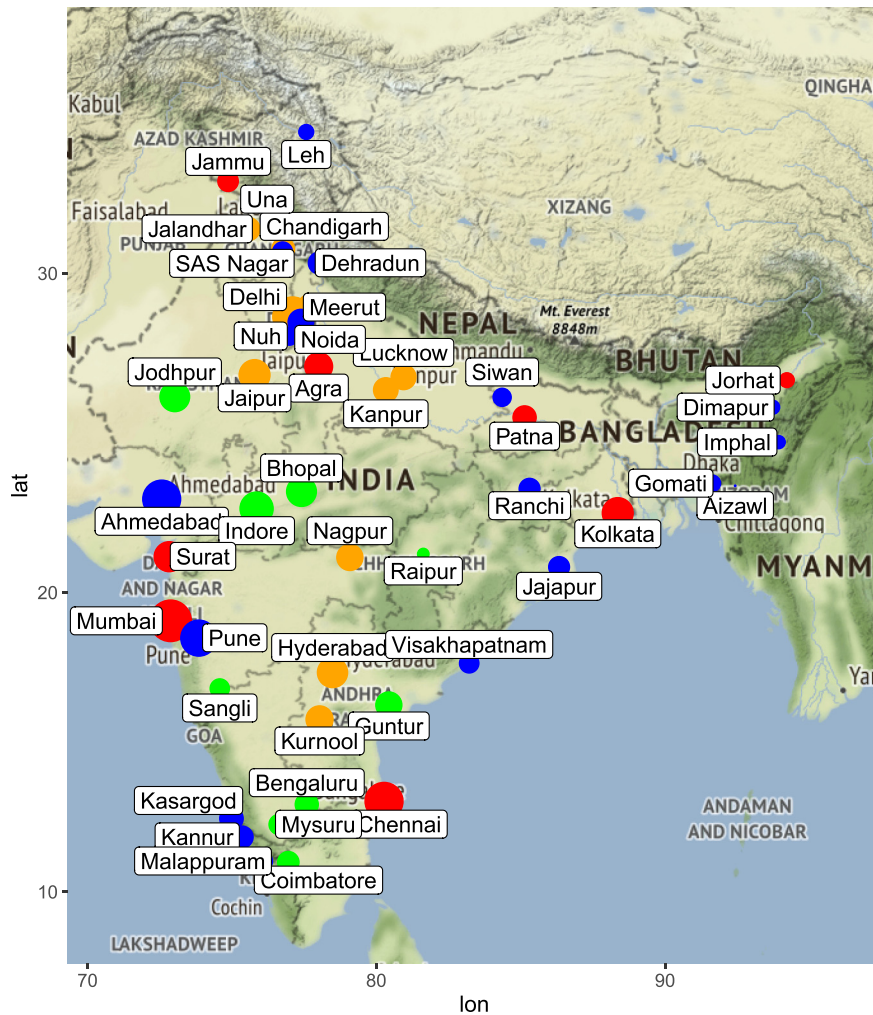


Fig. 1. Geographical spread, COVID-19 case counts and population density of the study locations. Selected locations are shown as bubbles, the size of which is proportional to log of COVID-19 case counts. The color of the bubble indicates quartile of population density based on the cutoffs mentioned in Supplementary Table 1 – first quartile, blue; second quartile, green, third quartile orange and fourth quartile, red.

cumulative COVID-19 cases till May 31, 2020 were 182,140. Thus, our selected geographic locations accounted for ~60% of all India COVID-19 cases till May 31, 2020. The top 5 contributing locations to the overall cumulative COVID-19 case counts were Mumbai (37666), Delhi (18058), Chennai (12040), Ahmedabad (11919) and Pune (7459) as shown in Supplementary Fig. 1.

3.2. Average estimated R_0 for COVID-19

We first estimated the R_0 based on case counts reported for the entire country as well as only for the locations included in this study. For each of these datasets, we estimated the R_0 in two ways – first based on the actual reported case counts and second by inflating the case counts to account for the potential underreporting on each day. The results of these analyses are shown in Fig. 2 and referred to as unadjusted (actual case counts, blue bars) and adjusted (for potential underreporting, purple bars). Our average estimates of R_0 using different methods of estimation and with or without adjusting for underreporting ranged from 1.18 to 1.27 for India and 1.15 to 1.28 for the selected study locations. All the estimates and their 95% confidence intervals (error bars in Fig. 2) were significantly above unity. Thus, the average estimates of R_0 were significantly greater than one, confirming the existence of the epidemic; the average R_0 estimates were only moderately above unity; the average R_0 estimates were

minimally influenced by potential underreporting; and that the study locations yielded average R_0 estimates consistent with those for the whole country thereby indirectly reaffirming the representativeness of the selected study locations.

We also examined the heterogeneity of the average R_0 estimates across the study locations. For these analyses, we restricted the locations which showed at least seven consecutive days with a contiguous segment of non-zero cases. Total of 35 locations were eligible based on this criterion. The average R_0 estimates derived using the ML method [point estimates and confidence intervals (CI)] for these 35 locations are shown in Table 1. There was a significant heterogeneity in the average R_0 estimates ($Q = 224.28$, degrees of freedom = 34, $p = 6.9 \times 10^{-30}$) with estimates ranging from 1.98 for Dehradun to 0.89 for Kolkata. The average R_0 estimates for the top five contributing locations were: Mumbai 1.16 (95% CI 1.14–1.18); Delhi 1.25 (95% CI 1.23–1.28); Chennai 1.20 (95% CI 1.17–1.23); Ahmedabad 1.10 (95% CI 1.07–1.13) and Pune 1.22 (95% CI 1.18–1.26).

We examined the potential association of geographical characteristics with the estimated R_0 . For this we conducted a multivariable regression model which included population density (a composite variable that includes information on population and area), elevation, latitude and longitude (to test for any cline effect). The results of these analyses are shown in Table 2. These results showed that none of the correlates was significantly associated with the estimated R_0 .

Table 1
Geographical characteristics of and COVID-19 transmission in selected locations across India.

Location	Adm unit	Population 2011	Latitude	Longitude	Area (km ²)	Elevation (m)	Population density (×1000/km ²)	PDQ ^a	COVID-19 cases (n)	Average R ₀ (95% CI) ^b
Agra	City	1,585,704	27.1767	78.0081	87.00	170.98	18.23	4	881	1.04 (0.95–1.14)
Ahmedabad	District	7,214,225	23.0225	72.5714	8106.70	53.03	0.89	1	11,919	1.10 (1.07–1.13)
Aizawl	City	293,416	23.4338	92.4304	455.84	1131.97	0.64	1	1	Unestimable ^c
Bengaluru	District	9,621,551	12.9716	77.5946	2196.32	920.45	4.38	2	260	1.17 (0.88–1.46)
Bhopal	City	1,798,218	23.2599	77.4126	285.88	526.97	6.29	3	1478	1.10 (1.02–1.18)
Chandigarh	UT	1,055,450	30.7333	76.7794	113.96	320.94	9.26	3	241	1.09 (0.90–1.29)
Chennai	District	7,088,000	13.0827	80.2707	426.06	6.10	16.64	4	12,040	1.20 (1.17–1.23)
Coimbatore	City	1,601,438	11.0168	76.9558	246.75	410.85	6.49	3	167	Unestimable
Dehradun	City	578,420	30.3165	78.0322	259.00	447.12	2.23	2	204	1.98 (1.55–2.42)
Delhi	UT	16,787,941	28.7041	77.1025	1484.07	224.02	11.31	4	18,058	1.25 (1.23–1.28)
Dimapur	City	254,674	25.9091	93.7266	121.73	145.08	2.09	2	26	Unestimable
Gomati	District	429,237	23.5167	91.6372	1522.79	24.08	0.28	1	49	Unestimable
Guntur	District	743,354	16.3067	80.4365	159.47	32.92	4.66	2	558	1.11 (0.97–1.25)
Hyderabad	City	6,809,970	17.385	78.4867	624.19	541.91	10.91	4	1630	1.30 (1.20–1.41)
Imphal	City	268,243	24.817	93.9368	556.85	786.04	0.48	1	20	Unestimable
Indore	City	1,994,397	22.7168	75.8577	518.00	548.61	3.85	2	3467	1.09 (1.03–1.14)
Jaipur	City	3,046,189	26.9124	75.7873	466.20	430.97	6.53	3	1937	1.05 (0.98–1.11)
Jajapur	District	37,458	20.8341	86.3326	2887.85	331.00	0.01	1	146	1.15 (0.83–1.47)
Jalandhar	City	873,725	31.326	75.5762	110.00	227.98	7.94	3	254	1.38 (1.07–1.69)
Jammu	City	502,197	32.73	74.87	26.65	350.50	18.84	4	132	1.46 (1.02–1.89)
Jodhpur	City	1,056,191	26.2389	73.0243	214.48	231.03	4.92	3	1434	1.09 (1.01–1.17)
Jorhat	City	153,889	26.75	94.22	12.59	116.12	12.23	4	31	Unestimable
Kannur	District	2,523,003	11.8689	75.3555	2965.55	0.91	0.85	1	198	1.38 (1.78–1.97)
Kanpur	City	2,767,348	26.4499	80.3319	403.70	125.88	6.85	3	377	0.98 (0.83–1.12)
Kasargod	District	1,307,375	12.4996	74.9869	1991.71	18.90	0.66	1	287	1.32 (0.98–1.67)
Kolkata	City	4,496,694	22.5726	88.3639	205.00	9.14	21.94	4	1952	0.89 (0.83–0.96)
Kurnool	City	457,633	15.8281	78.0373	69.52	274.00	6.58	3	715	1.07 (0.96–1.19)
Leh	City	30,870	34.1526	77.5771	45.12	3505.03	0.68	1	32	Unestimable
Lucknow	City	2,817,105	26.8467	80.9462	349.65	123.13	8.06	3	424	1.19 (0.95–1.43)
Malappuram	City	101,386	11.051	76.0711	33.62	101.80	3.02	2	102	1.53 (1.01–2.05)
Meerut	City	1,524,908	28.9845	77.7064	183.89	224.63	8.29	3	501	1.18 (1.02–1.33)
Mumbai	City	12,478,447	19.076	72.8777	603.47	14.02	20.68	4	37,666	1.16 (1.14–1.18)
Mysuru	City	920,550	12.2958	76.6394	155.71	762.88	5.91	3	129	Unestimable
Nagpur	City	2,405,665	21.1458	79.0882	227.35	310.88	10.58	4	573	1.14 (1.00–1.28)
Noida	City	637,232	28.5355	77.391	202.02	213.35	3.15	2	487	1.23 (1.05–1.40)
Nuh	District	1,089,263	25.5941	85.1376	1859.62	199.02	0.59	1	70	Unestimable
Patna	City	1,695,000	25.5941	85.1376	98.42	53.03	17.22	4	268	1.12 (0.92–1.32)
Pune	District	9,429,408	18.5204	73.8567	15,641.01	560.80	0.60	1	7459	1.22 (1.18–1.26)
Raipur	City	1,010,087	21.2514	81.6296	173.53	298.08	5.82	3	13	Unestimable
Ranchi	City	1,073,440	23.3441	85.3096	652.03	651.02	1.65	2	148	1.06 (0.79–1.33)
Sangli	City	502,793	16.8524	74.5815	118.80	548.92	10.96126	2	97	1.19 (0.81–1.56)
SAS Nagar	District	994,628	30.7046	76.7179	1098.16	316.06	2.345821	1	112	1.30 (1.20–1.41)
Siwan	City	135,066	26.22	84.36	69.41	71.93	5.039776	2	73	1.07 (0.62–2.11)
Surat	City	4,467,797	21.1702	72.8311	326.52	13.11	35.43902	4	1569	1.12 (1.04–1.20)
Una	District	521,173	17.6868	83.2185	1541.05	369.09	0.875921	1	22	Unestimable
Vishakapatnam	City	2,035,922	17.6868	83.2185	697.95	45.11	7.555002	2	101	1.27 (0.86–1.67)

^a Quartile of population density.

^b Estimated using the maximum likelihood method.

^c Contiguous epidemic period <7 days.

3.3. Temporal changes in R₀ estimates

Next, we considered the variability in R₀ estimates over the duration of the study for all locations together. Fig. 3 shows that the R₀ estimates were initially high but undulated widely and gradually converged towards the overall estimates shown in Fig. 2 with narrow confidence bands later. Thus, the time dependent R₀ estimates showed considerable variation across study time.

We examined the association of the time-dependent R₀ estimates with two socio-behavioral characteristics – implementation of a countrywide lockdown and the extent of social distancing as reflected by the cellphone mobility data. When contrasted against the various phases of countrywide lockdown in India (grey shaded regions in Fig. 3), we found that the median R₀ estimates consistently reduced as lockdown was imposed. Before the lockdown began (March 1 through March 24, 2020) the median R₀ was 1.54 and this estimate decreased to 1.40 (March 25–April 14, 2020), 1.21 (April 15–May 3, 2020), 1.16 (May 4–May 17, 2020) and 1.10 (May 18, 2020 onwards) during the lockdown phases 1 through 4, respectively (Kruskal-Wallis *p* < 0.0001).

The cellphone-based community mobility data also revealed consistent and interesting patterns. As shown in Supplementary Fig. 2, the overall trends in community mobility for all five destinations showed a dramatic decrease around the beginning of phase 1 lockdown, remained very low during phase 1 lockdown and then gradually increased as the lockdown progressed. The 5-day rolling z-scores for the average mobility based on these five parameters is shown in Fig. 3 (green curve). This curve showed a dramatic reduction in mobility just prior to and during the first two phases of the lockdown. The curve showed an increasing trend in phases 2 and 4 of the lockdown.

3.4. Association of time dependent R₀ estimates with meteorological data

The time trends for air temperature, relative humidity, air pressure, wind speed and rainfall are shown in Fig. 4A. Over the duration of the study, air temperature and wind speed steadily increased; relative humidity and air pressure gradually decreased while rainfall remained steady. As a first step of the association analyses, we estimated the cross-correlation between each meteorological variables and the R₀ estimates. Fig. 4B shows the cross-correlograms for lags ranging from –10

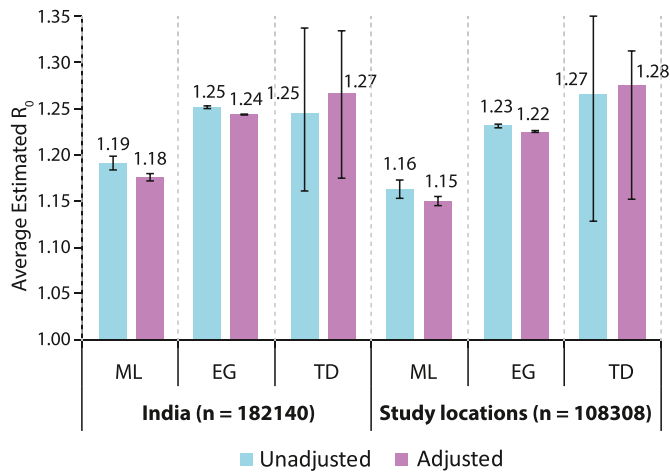


Fig. 2. Average estimated R_0 for COVID-19. Bars show the average R_0 estimates and error bars indicate the 95% confidence intervals. Average R_0 estimates were derived using three methods: ML, maximum likelihood; EG, exponential growth; and TD, time dependent. Each estimate was also derived without adjustment (unadjusted, blue bars) and adjusted for potential underestimation (adjusted, purple bars).

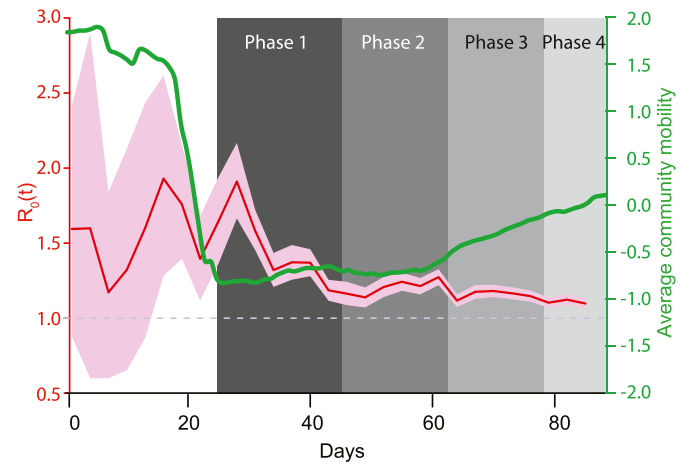


Fig. 3. Time dependent R_0 and socio-behavioral interventions. Red line and pink bands indicate the time dependent R_0 and 95% confidence intervals, respectively, for each day during the study. These align to the left axis (colored red). The green curve shows the 5-day rolling average z-score for cellphone-based mobility data and aligns to the right axis (colored green). Shaded boxes in the background indicate different phases of the countrywide lockdown in India.

to 10 days. We found that higher temperature, wind speed and rainfall were correlated inversely while relative humidity and air pressure were correlated positively with time dependent R_0 estimates. The best cross-correlation was observed for temperature and humidity on the same day (-0.73 and 0.63 , respectively), wind speed on previous day (-0.40), rainfall preceding by 4 days (-0.29) and air pressure preceding by 6 days (0.54). Together these results indicated that concurrent or immediately preceding values of meteorological variables are significantly correlated with time dependent R_0 estimates.

3.5. Multivariable association of meteorological and socio-behavioral predictors with time dependent R_0

We then examined whether the meteorological and socio-behavioral covariates were independently associated with time dependent R_0 estimates. The full regression model used time dependent R_0 estimates as the dependent variable and following 14 covariates as explanatory variables: five z-scores for the meteorological covariates, five z-scores for community mobility data and four phases of lockdown (each used as a dichotomous variable). The results of these analyses are shown in Table 3. In the full model, we observed that the lockdown phases 3 (only marginally) and 4 and wind speed were the only covariates that were statistically significantly associated with R_0 estimates. In this context, the mobility data (which was highly correlated with the lockdown phases) did not retain statistical significance. However, considering the potential for interactions among covariates and the possibility of an underpowered full model (14 covariates observed on 92 days), we conducted stepwise regression modeling with a probability retention criterion of 0.05. The results of the final model (Table 3) showed that air temperature z-score, wind speed z-score and lockdown

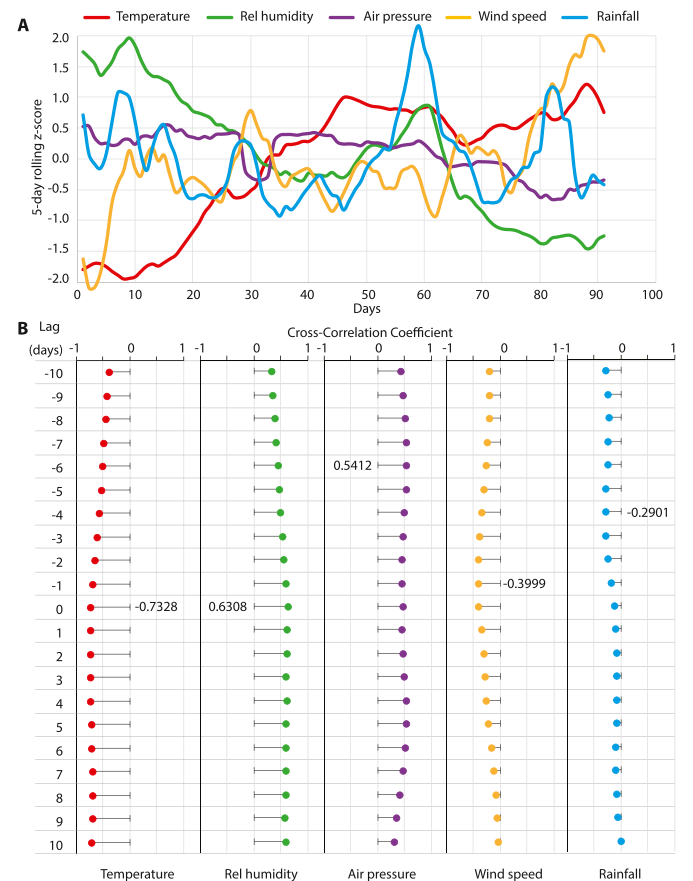


Fig. 4. Meteorological determinants of COVID-19 transmissibility. (A) Time trends for each of the five, color-coded meteorological variables. For each variable, the data were first z-transformed and then subjected to a 5-day moving average. (B) Cross-correlograms for correlation of each meteorological variable with estimated time dependent R_0 . All cross-correlograms were assessed between lags of -10 to 10 days. Most significant correlation for each variable is indicated as a number alongside the lag at which it was observed. Rel, relative.

Table 2
Association of geographical characteristics with estimated R_0 . The full model used inverse variance weighting to account for variability in R_0 estimates.

Covariate	β	95% CI	P
Population density	0.0017	$-0.0025-0.0060$	0.408
Elevation	0.0001	$-0.0001-0.0003$	0.232
Latitude	-0.0002	$-0.0066-0.0062$	0.944
Longitude	-0.0034	$-0.0115-0.0046$	0.392

β , regression coefficient; CI, confidence interval; p, significance value.

Table 3

Multivariable association of meteorological and socio-behavioral covariates with time dependent R_0 estimates (all study locations, March 1–May 31, 2020).

Covariate	β	95% CI	p
Full model			
Temperature z-score	−0.10	−0.24–0.05	0.190
Relative humidity z-score	−0.04	−0.16–0.09	0.539
Air pressure z-score	−0.06	−0.18–0.06	0.322
Wind speed z-score	0.06	0.00–0.11	0.036
Rainfall z-score	0.02	−0.03–0.07	0.471
Retail/recreation z-score	0.54	−0.30–1.37	0.204
Grocery/pharmacy z-score	0.17	−0.08–0.41	0.184
Parks z-score	−0.26	−0.91–0.39	0.426
Transit station z-score	−0.48	−1.18–0.23	0.180
Workplaces z-score	0.04	−0.19–0.28	0.724
Lockdown phase 1	−0.01	−0.27–0.25	0.936
Lockdown phase 2	−0.23	−0.61–0.16	0.247
Lockdown phase 3	−0.41	−0.87–0.05	0.079
Lockdown phase 4	−0.61	−1.14 to −0.08	0.024
Intercept	1.56	1.30–1.81	<0.001
Final model			
Temperature z-score	−0.08	−0.13 to −0.03	0.005
Wind speed z-score	0.08	0.03–0.12	0.003
Lockdown phase 2	−0.22	−0.34 to −0.09	0.001
Lockdown phase 3	−0.32	−0.45 to −0.19	<0.001
Lockdown phase 4	−0.47	−0.63 to −0.30	<0.001
Intercept	1.51	1.44–1.58	<0.001

β , regression coefficient; CI, confidence interval; p, significance value.

phases 2–4 were retained in the final model. This model fitted the data well with an adjusted R^2 of 0.56 (Supplementary Fig. 3).

From the point of public health relevance, we then quantified the contribution of each variable retained in the final model to the overall variance of time dependent R_0 . The PRE estimates for the variables retained in the final model were as follows: air temperature: 9.1%, wind speed: 9.9%, lockdown phase 2: 12.2%, lockdown phase 3: 22.5% and lockdown phase 4: 27.0%. These results indicate that while the meteorological factors of air temperature and wind speed were statistically significant predictors of COVID-19 transmissibility, their contribution to dampening the R_0 estimate was 3–4 times weaker as compared to the countrywide lockdown phases 2–4.

4. Discussion

Using nationally representative data from India over a three-month period, our study made three cardinal observations. First, the average basic reproduction rate (R_0) of COVID-19 infection in the period from March 1 through May 31, 2020 ranged from 1.15 to 1.28 even after accounting for the potential undertesting. Second, the COVID-19 transmissibility was significantly associated with daily average air temperature (inversely), daily average wind speed (positively) and the countrywide intervention of lockdown (inversely). Third, the contribution of lockdown to the variability in time dependent R_0 was three times more than the contribution of air temperature and wind speed combined. We did not observe a statistically significant association of any geographic characteristic with R_0 . Together, these results suggest that in India while the meteorological determinants of COVID-19 were independently associated with the transmissibility, their contribution was outweighed by that of the countrywide lockdown.

Even though statistically significantly greater than unity, our estimate of R_0 was low. This estimate is comparable to the value of 1.32 reported by others (Du et al., 2020). However, the low value of R_0 should be interpreted with caution. First, there has been a debate about the length of serial interval with values ranging from as low as 3 days to as high as 9 days (Du et al., 2020; Ganyani et al., 2020; Moradi and Eshtrati, 2020; Nishiura et al., 2020; Zhang et al., 2020). We used the serial interval of ~4 days which is on the lower side of

the reported range and could have partly contributed to the low R_0 observed in this study. Second, the major part of the study period included lockdown and reduced mobility and therefore the R_0 estimate may represent a muted transmissibility owing to interventions in place. Third, the low R_0 estimate does not indicate lack of viral infectiousness or any other viral characteristic but only implies the extent of potential spread of the disease (Delamater et al., 2019). Fourth, the epidemic of COVID-19 is still ongoing and our estimate of R_0 only captures the initial, ascending limb of the epidemic curve. Therefore, this R_0 estimate does not fully capture the population dynamics of COVID-19. Fifth, our estimate of R_0 is a conglomerate of the varying estimates across the study locations as shown in Table 1. The variability in R_0 across study locations indicates that the location-specific epidemic curves were not aligned to the same starting point in time and therefore our R_0 estimate should not be used as a generalizable estimate of COVID-19 transmissibility. The reason for estimating R_0 in the study was to investigate the potential influence of geo-meteorological factors on transmissibility.

Several researchers around the world have demonstrated an inverse relationship between air temperature and number of COVID-19 cases (Demongeot et al., 2020; Guo et al., 2020; Harmooshi et al., 2020; Jahangiri et al., 2020; Malki et al., 2020; Pramanik et al., 2020; Ran et al., 2020; Ren et al., 2020; Seligmann et al., 2020a; Steiger et al., 2020). Our results are in agreement with the general understanding that higher ambient temperature can inversely influence COVID-19 transmissibility (Guo et al., 2020; Jahangiri et al., 2020). Our study duration marks a period of increasing temperature in the Indian peninsula and our results indicate that, in general, high ambient temperatures were associated with lower R_0 estimates such that one standard deviation increase in air temperature was associated with a 0.08 lower R_0 (Table 3, final model). It has been shown that increased air temperature is associated with surface inactivation and reduced transmissibility of the coronavirus (Biryukov et al., 2020; Ren et al., 2020). An elegant review (Shakil et al., 2020) has noted that most of the studies on the association of air temperature with COVID-19 transmission have emerged from areas where temperatures are not high and therefore more studies from high-temperature areas are needed. Our study therefore furthers the published literature on the association of air temperature and COVID-19 transmission.

On the other hand, we observed that a unit standard deviation increase in wind speed was associated with a 0.08 higher R_0 (Table 3, final model). The current evidence for the potential role of wind speed in COVID-19 spread is conflicting with studies reporting positive (Sahin, 2020), null (Bashir et al., 2020; Su et al., 2020; Zoran et al., 2020) and negative (Adhikari and Yin, 2020; Ahmadi et al., 2020) association with COVID-19 transmissibility. Our observation of a positive association of COVID-19 transmissibility with wind speed is in line with the growing idea that the SARS-CoV-2 virus may be airborne. (Carraturo et al., 2020; Wilson et al., 2020) Of note, incidence of COVID-19 has been shown to be associated with air pollution (Adhikari and Yin, 2020; Faridi et al., 2020; Sharma and Balyan, 2020) – a factor that is significantly influenced by wind speed (Zhang, 2019). Arguably, aerosol concentration can be reduced by high wind speeds, diluting the potential dose of infection and thus reducing the transmissibility (Eslami and Jalili, 2020). On the other hand, moderate wind speed combined with high number of susceptible individuals can lead to an effective dispersion of the aerosols and may lead to a positive association between wind speed and COVID-19 transmissibility (Sahin, 2020). Our study cannot directly answer these interesting hypotheses, which should be tested in future studies. Knowledge of the biophysical aspects of observed ecological associations is mechanistically important and should be the focus of future studies.

Nonetheless, a head-to-head comparison indicated that the lockdown period was associated with three times stronger contribution to the variability in R_0 as compared to that of air temperature and wind speed combined. From the perspective of public health action, this

observation supports the role of proactive interventions to de-escalate the transmissibility of COVID-19. Conceivably, as the air temperature wanes and the lockdown eases, more cases of COVID-19 can be expected.

There is both a logical and biological support to expect a positive correlation between population density and COVID-19 transmission (Amoo et al., 2020; Jahangiri et al., 2020; Liu, 2020; Rashed et al., 2020; Rocklov and Sjodin, 2020; Tammes, 2020). Our study failed to show an association between population density and COVID-19 transmissibility in a regression framework. There could be several explanations that partly account for the observed lack of association between population density and COVID-19 transmission. First, the geographical locations represented a more global than focal population density which will be immediate concern in COVID-19 transmission. Second, the duration of epidemic was not the same across all the locations studied – locations in the lowest quartile of population density had an average observed duration of only 11 days while those in the highest quartile of population density had an average of 6 weeks of epidemic experience. A direct comparison of transmissibility across gradients of population density can therefore be confounded. Third, travel history – a major determinant of COVID-19 transmission (Cruz et al., 2020; Nussbaumer-Streit et al., 2020) – was not included in this study. Conceivably, travel is more frequent to the metropolitan areas with high population density and therefore the epidemic will be slower to take off in low density locations. Together, these possibilities make it difficult to tease apart the potential role of population density in our study.

Our results should be interpreted in the light of some limitations. First, this was a retrospective analysis that combined data from different sources. The data are collected at the level of geographic locations and not at the level of individual patient. For example, person-to-person transmissibility of COVID-19 in an infector-infectee scenario was not investigated in this study. Therefore, all the estimates and associations should only be considered as general patterns rather than definitive evidence. Second, akin to any observational study, unmeasured confounding can be expected to be operational. Third, it may appear surprising that the cross-correlations in time series analyses (Fig. 4B) for air temperature, relative humidity and wind speed that highest values were on (or very close to) the day of time-dependent R_0 . It should be noted that the cross-correlation shown in Fig. 4B are for 5-day smoothed weather parameters. Still, our study generates the hypothesis that while the case counts in response to environmental fluctuations may take time to be altered, it is possible that the influence on transmissibility (R_0) is more immediate. Future studies need to specifically address this hypothesis.

We would like to stress that the observations made in this study relate to the initial spread of COVID-19 in India. As the epidemic enters subsequent phases, these observations and patterns can change. Such change of observed associations has been reported with regard to association with air temperature (Seligmann et al., 2020a), altitude (Seligmann et al., 2020b) and population density (Seligmann et al., 2020a). For example, based on data from 124 countries in the early phase and 28 countries in the second phase of COVID-19 epidemic, it was reported that COVID-19 transmission decreased with air temperature in the early phase but an inverse trend was observed during the second phase (Seligmann et al., 2020a). This observation has been attributed to the mutant and better-adapted viruses that sprang the second wave of COVID-19 transmission. The observations we report in this study refer to the initial phase and are consistent with the early phase observations despite these potential limitations our study demonstrated interesting and important patterns of association of geo-meteorological factors in COVID-19 spread. To control a pandemic of the current magnitude, all scientific evidence from a holistic standpoint is needed. To that end, our study provides clues into the ecological aspects of COVID-19 during the initial months in India.

CRediT authorship contribution statement

Hemant Kulkarni: Conceptualization, Data curation, Formal analyses, Writing; **Harshwardhan V Khandait:** Data curation, Review; **Uday W Narlawar:** Conceptualization, Reviewing, Editing; **Pragati G Rathod:** Conceptualization, Writing; **Manju Mamtani:** Conceptualization, Artwork, Writing, Review.

Declaration of competing interest

The authors declare that they have no conflicts of interest to declare.

Appendix A. Supplementary data

Supplementary data to this article can be found online at <https://doi.org/10.1016/j.scitotenv.2020.142801>.

References

- Adhikari, A., Yin, J., 2020. Short-term effects of ambient ozone, PM_{2.5}, and meteorological factors on COVID-19 confirmed cases and deaths in Queens, New York. *Int. J. Environ. Res. Public Health* 17.
- Ahmadi, M., Shariifi, A., Dorosti, S., Jafarzadeh Ghouschi, S., Ghanbari, N., 2020. Investigation of effective climatology parameters on COVID-19 outbreak in Iran. *Sci. Total Environ.* 729, 138705.
- Amoo, E.O., Adekeye, O., Olawole-Isaac, A., Fasina, F., Adekola, P.O., Samuel, G.W., et al., 2020. Nigeria and Italy divergences in coronavirus experience: impact of population density. *Sci. World J.* 2020, 8923036.
- Bashir, M.F., Ma, B., Bilal, Komal, B., Bashir, M.A., Tan, D., et al., 2020. Correlation between climate indicators and COVID-19 pandemic in New York, USA. *Sci. Total Environ.* 728, 138835.
- Biryukov, J., Boydston, J.A., Dunning, R.A., Yeager, J.J., Wood, S., Reese, A.L., et al., 2020. Increasing temperature and relative humidity accelerates inactivation of SARS-CoV-2 on surfaces. *mSphere* 5.
- Brassley, J., Heneghan, C., Mahtani, K.R., Aronson, J.K., 2020. Do Weather Conditions Influence the Transmission of the Coronavirus (SARS-CoV-2)? Centre for Evidence-Based Medicine, Nuffield and Department of Primary Care Health Sciences, University of Oxford, Oxford, London
- Briz-Redon, A., Serrano-Aroca, A., 2020. A spatio-temporal analysis for exploring the effect of temperature on COVID-19 early evolution in Spain. *Sci. Total Environ.* 728, 138811.
- Carraturo, F., Del Giudice, C., Morelli, M., Cerullo, V., Libralato, G., Galdiero, E., et al., 2020. Persistence of SARS-CoV-2 in the environment and COVID-19 transmission risk from environmental matrices and surfaces. *Environ. Pollut.* 265, 115010.
- Cruz, C.J.P., Ganly, R., Li, Z., Gietel-Basten, S., 2020. Exploring the young demographic profile of COVID-19 cases in Hong Kong: evidence from migration and travel history data. *PLoS One* 15, e0235306.
- Das, K., Chatterjee, N.D., 2020. Examine the impact of weather and ambient air pollutant parameters on daily case of COVID-19 in India. *medRxiv* <https://doi.org/10.1101/2020.06.08.20125401> (2020.06.08.20125401).
- Delamater, P.L., Street, E.J., Leslie, T.F., Yang, Y.T., Jacobsen, K.H., 2019. Complexity of the basic reproduction number (R_0). *Emerg. Infect. Dis.* 25, 1–4.
- Demongeot, J., Flet-Berliac, Y., Seligmann, H., 2020. Temperature decreases spread parameters of the new Covid-19 case dynamics. *Biology (Basel)* 9.
- Du, Z., Xu, X., Wu, Y., Wang, L., Cowling, B.J., Meyers, L.A., 2020. Serial interval of COVID-19 among publicly reported confirmed cases. *Emerg. Infect. Dis.* 26, 1341–1343.
- Eslami, H., Jalili, M., 2020. The role of environmental factors to transmission of SARS-CoV-2 (COVID-19). *AMB Express* 10, 92.
- Faridi, S., Niazi, S., Sadeghi, K., Naddafi, K., Yavarian, J., Shamsipour, M., et al., 2020. A field indoor air measurement of SARS-CoV-2 in the patient rooms of the largest hospital in Iran. *Sci. Total Environ.* 725, 138401.
- Ganyani, T., Kremer, C., Chen, D., Torneri, A., Faes, C., Wallinga, J., et al., 2020. Estimating the generation interval for coronavirus disease (COVID-19) based on symptom onset data, March 2020. *Euro Surveill* 25.
- Guo, X.J., Zhang, H., Zeng, Y.P., 2020. Transmissibility of COVID-19 in 11 major cities in China and its association with temperature and humidity in Beijing, Shanghai, Guangzhou, and Chengdu. *Infect. Dis. Poverty* 9, 87.
- Gupta, A., Pradhan, B., 2020. Impact of daily weather on COVID-19 outbreak in India. *medRxiv* <https://doi.org/10.1101/2020.06.15.20131490> (2020.06.15.20131490).
- Harmooshi, N.N., Shirbandi, K., Rahim, F., 2020. Environmental concern regarding the effect of humidity and temperature on 2019-nCoV survival: fact or fiction. *Environ. Sci. Pollut. Res. Int.* 27 (29), 36027–36036. <https://doi.org/10.1007/s11356-020-09733-w>.
- Jahangiri, M., Jahangiri, M., Najafgholipour, M., 2020. The sensitivity and specificity analyses of ambient temperature and population size on the transmission rate of the novel coronavirus (COVID-19) in different provinces of Iran. *Sci. Total Environ.* 728, 138872.
- Judd, C.M., McClelland, G.H., Ryan, C.S., 2009. *Data Analysis: A Model Comparison Approach*. Taylor & Francis Group, Routledge.
- Lachmann, A., Jagodnik, K.M., Giorgi, F.M., Ray, F., 2020. Correcting under-reported COVID-19 case numbers: estimating the true scale of the pandemic. *medRxiv* <https://doi.org/10.1101/2020.03.14.20036178> (2020.03.14.20036178).

- Liu, L., 2020. Emerging study on the transmission of the novel coronavirus (COVID-19) from urban perspective: evidence from China. *Cities* 103, 102759.
- Malki, Z., Atlam, E.S., Hassanien, A.E., Dagnew, G., Elhosseini, M.A., Gad, I., 2020. Association between weather data and COVID-19 pandemic predicting mortality rate: machine learning approaches. *Chaos, Solitons Fractals* 138, 110137.
- Moradi, Y., Eshrati, B., 2020. Estimation of the net reproductive number of COVID-19 in Iran. *Med. J. Islam Repub. Iran* 34, 34.
- Nishiura, H., Linton, N.M., Akhmetzhanov, A.R., 2020. Serial interval of novel coronavirus (COVID-19) infections. *Int. J. Infect. Dis.* 93, 284–286.
- Nussbaumer-Streit, B., Mayr, V., Dobrescu, A.I., Chapman, A., Persad, E., Klerings, I., et al., 2020. Quarantine alone or in combination with other public health measures to control COVID-19: a rapid review. *Cochrane Database Syst. Rev.* 4, CD013574.
- Obadia, T., Haneef, R., Boelle, P.Y., 2012. The R0 package: a toolbox to estimate reproduction numbers for epidemic outbreaks. *BMC Med. Inform. Decis. Mak.* 12, 147.
- Pramanik, M., Udmale, P., Bisht, P., Chowdhury, K., Szabo, S., Pal, I., 2020. Climatic factors influence the spread of COVID-19 in Russia. *Int. J. Environ. Health Res.* 1–15.
- Prata, D.N., Rodrigues, W., Bermejo, P.H., 2020. Temperature significantly changes COVID-19 transmission in (sub)tropical cities of Brazil. *Sci. Total Environ.* 729, 138862.
- Qi, H., Xiao, S., Shi, R., Ward, M.P., Chen, Y., Tu, W., et al., 2020. COVID-19 transmission in Mainland China is associated with temperature and humidity: a time-series analysis. *Sci. Total Environ.* 728, 138778.
- Ran, J., Zhao, S., Han, L., Liao, G., Wang, K., Wang, M.H., He, D., 2020. A re-analysis in exploring the association between temperature and COVID-19 transmissibility: an ecological study with 154 Chinese cities. *Eur. Respir. J.* 56 (2), 2001253. <https://doi.org/10.1183/13993003.01253-2020>.
- Rashed, E.A., Koderia, S., Gomez-Tames, J., Hirata, A., 2020. Influence of absolute humidity, temperature and population density on COVID-19 spread and decay durations: multi-prefecture study in Japan. *Int. J. Environ. Res. Public Health* 17.
- Ren, S.Y., Wang, W.B., Hao, Y.G., Zhang, H.R., Wang, Z.C., Chen, Y.L., et al., 2020. Stability and infectivity of coronaviruses in inanimate environments. *World J. Clin. Cases* 8, 1391–1399.
- Rocklöv, J., Sjödin, H., 2020. High population densities catalyse the spread of COVID-19. *J. Travel. Med.* 27.
- Sahin, M., 2020. Impact of weather on COVID-19 pandemic in Turkey. *Sci. Total Environ.* 728, 138810.
- Seligmann, H., Iggui, S., Rachdi, M., Vuillerme, N., Demongeot, J., 2020a. Inverted covariate effects for first versus mutated second wave Covid-19: high temperature spread biased for young. *Biology (Basel)* 9.
- Seligmann, H., Vuillerme, N., Demongeot, J., 2020b. Summer COVID-19 third wave: faster high altitude spread suggests high UV adaptation. *medRxiv* <https://doi.org/10.1101/2020.08.17.20176628> (2020.08.17.20176628).
- Shakil, M.H., Munim, Z.H., Tasnia, M., Sarowar, S., 2020. COVID-19 and the environment: a critical review and research agenda. *Sci. Total Environ.* 745, 141022.
- Sharma, A.K., Balyan, P., 2020. Air pollution and COVID-19: is the connect worth its weight? *Indian J. Public Health* 64, S132–S134.
- Shi, P., Dong, Y., Yan, H., Zhao, C., Li, X., Liu, W., et al., 2020. Impact of temperature on the dynamics of the COVID-19 outbreak in China. *Sci. Total Environ.* 728, 138890.
- Singh, K., Agarwal, A., 2020. Impact of weather indicators on the COVID-19 outbreak: a multi-state study in India. *medRxiv* <https://doi.org/10.1101/2020.06.14.20130666> (2020.06.14.20130666).
- Steiger, E., Musgnug, T., Kroll, L.E., 2020. Causal analysis of COVID-19 observational data in German districts reveals effects of mobility, awareness, and temperature. *medRxiv* <https://doi.org/10.1101/2020.07.15.20154476> (2020.07.15.20154476).
- Su, D., Chen, Y., He, K., Zhang, T., Tan, M., Zhang, Y., et al., 2020. Influence of socio-ecological factors on COVID-19 risk: a cross-sectional study based on 178 countries/regions worldwide. *medRxiv* <https://doi.org/10.1101/2020.04.23.20077545>.
- Tammes, P., 2020. Social distancing, population density, and spread of COVID-19 in England: a longitudinal study. *BJGP Open* 4.
- Tosepu, R., Gunawan, J., Effendy, D.S., Ahmad, O.A.I., Lestari, H., Bahar, H., et al., 2020. Correlation between weather and Covid-19 pandemic in Jakarta, Indonesia. *Sci. Total Environ.* 725, 138436.
- Vantarakis, A., Chatziprodromidou, I., Apostolou, T., 2020. COVID-19 and environmental factors. A PRISMA-compliant systematic review. *medRxiv* <https://doi.org/10.1101/2020.05.10.20069732> (2020.05.10.20069732).
- Wilson, N.M., Norton, A., Young, F.P., Collins, D.W., 2020. Airborne transmission of severe acute respiratory syndrome coronavirus-2 to healthcare workers: a narrative review. *Anaesthesia* 75, 1086–1095.
- Yao, Y., Pan, J., Liu, Z., Meng, X., Wang, W., Kan, H., et al., 2020. No association of COVID-19 transmission with temperature or UV radiation in Chinese cities. *Eur. Respir. J.* 55.
- Zhang, Y., 2019. Dynamic effect analysis of meteorological conditions on air pollution: a case study from Beijing. *Sci. Total Environ.* 684, 178–185.
- Zhang, J., Litvinova, M., Wang, W., Wang, Y., Deng, X., Chen, X., et al., 2020. Evolving epidemiology of novel coronavirus diseases 2019 and possible interruption of local transmission outside Hubei Province in China: a descriptive and modeling study. *medRxiv* <https://doi.org/10.1101/2020.02.21.20026328>.
- Zoran, M.A., Savastri, R.S., Savastri, D.M., Tautan, M.N., 2020. Assessing the relationship between ground levels of ozone (O₃) and nitrogen dioxide (NO₂) with coronavirus (COVID-19) in Milan, Italy. *Sci. Total Environ.* 740, 140005.